Eur. Phys. J. D **34**, 311–313 (2005)
DOI: 10.1140/epjd/e2005-00102-1

THE EUROPEAN PHYSICAL JOURNAL D

The Coulomb instability of charged microdroplets: dynamics and scaling

T. Achtzehn, R. Müller, D. Duft, and T. Leisner[a]

Institut für Physik, TU Ilmenau, Postfach 100565, 98684 Ilmenau, Germany

Received 6 September 2004
Published online 13 July 2005

Abstract. The stability and disintegration dynamics of evaporating highly charged liquid droplets from ethylene glycol and glycerol is investigated by ultrafast microscopy and analyzed as a function of temperature and droplet size. In the moment of instability the droplets have deformed to elongated spindle like shapes from which pairs of opposite jets of highly charged liquid are emitted. The thickness of the jets and the shape of the deformed droplet are remarkably insensitive to the size and viscosity of the unstable droplet, while the speed of disintegration is found to scale with a power law for both variables, the exponent being close to 3/2.

PACS. 52.57.Fg Implosion symmetry and hydrodynamic instability (Rayleigh-Taylor, Richtmyer-Meshkov, imprint, etc.) – 47.20.-k Hydrodynamic stability – 36.40.Qv Stability and fragmentation of clusters

1 Introduction

The breakup of charged microdroplets is an important process for the charge separation in electrified clouds as well as in various technical applications like electrospray ionization, fuel injection or ink jet printing and has been studied theoretically as early as 1882 by Lord Rayleigh [1]. He concluded that for a drop with radius a_0, surface tension σ and charge Q the spherical shape remains stable as long as the fissility $X = Q^2/(64\pi^2\varepsilon_0\sigma a_0^3)$ is smaller than one. If X approaches unity, the quadrupole deformation is the first to become unstable. Rayleigh showed further that for X much larger than one, higher multipole deformations grow faster than the quadrupole mode. For such systems he predicted that the instability occurs via the formation of "fine jets, whose fineness, however, has a limit", without giving further comments. In several modern experiments, a droplet breakup below the Rayleigh limit was found [2–6]. In a series of recent experiments we have been able to show that for evaporating highly charged microdroplets of ethylene glycol, the instability occurs indeed exactly at $X = 1$ [7]. We furthermore could visualize the instability during its evolution and observed opposite pairs of liquid jets originating from the deformed droplets [8] (cf. Fig. 1). Similar jet formation has been reported for the breakup of neutral methanol droplets in high electric fields [9]. In this contribution we report on extended measurements performed for ethylene glycol and glycerol droplets at different droplet sizes and at variable temperatures. These experiments allow to assess the influence of droplet size and viscosity on the dynamics of the instability and might prove useful for the quantitative understanding of the dynamics of the jet formation process, which, despite of considerable effort [10–12], is not fully clear at the moment.

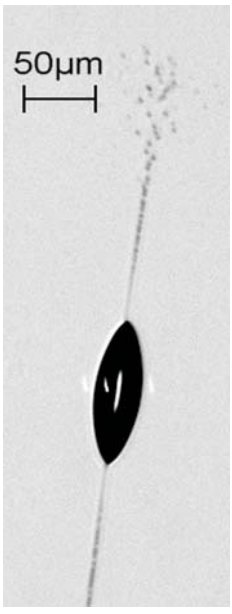

Fig. 1. Micro-photograph of a droplet of ethylene glycol in the moment of jet emission.

2 Experimental

Individual droplets of ethylene glycol were generated with a piezo driven nozzle (Microdrop, Fig. 2c), charged by influence from a high voltage electrode and injected into a

[a] e-mail: Thomas.Leisner@tu-ilmenau.de

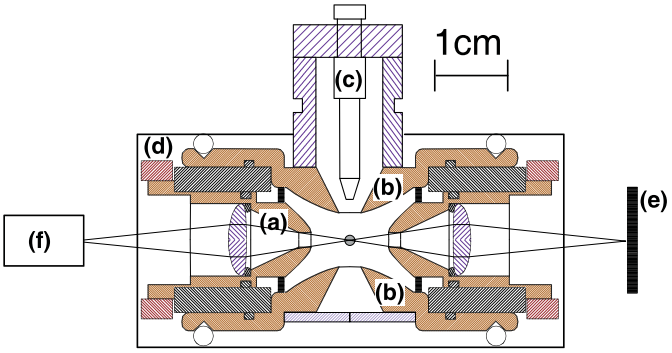

Fig. 2. Vertical cross-section of the levitator setup, for an explanation of the letters see text.

home built electrodynamic balance operating under ambient pressure. Here they evaporate until their limit of stability is reached. Then the instability is observed microscopically.

The balance is of the classical "Paul-trap" design [13,14]. A schematic cross section is given in Figure 2. It mainly consists of a hyperboloidal torus electrode (radius $r_0 = 5$ mm, Fig. 2a) and top and bottom hyperboloidal cap electrodes (Fig. 2b). The temperature is adjustable between room temperature and 400 K by resistive heating (Fig. 2d). The droplets are centered and levitated by applying a AC voltage with an amplitude of 1500 V and variable frequency to both endcap electrodes. A static field in vertical direction for the compensation of the gravitational force on the droplet is created by superimposing DC voltages of opposite sign to the top and bottom electrode. In order to observe the droplets, the balance is placed inside a horizontally oriented long working distance microscope (Mitutoyo, 10× and 20× objectives, not shown in Fig. 2). This microscope is equipped with a triggerable flash lamp (HSPS nanolight) for illumination and a cooled CCD camera (PCO Sensicam) for image acquisition. The size of the droplets can be determined from the microscope images within an error of ± 0.5 μm. The droplet is illuminated by a HeNe laser beam and imaged onto a vertically oriented linear CCD array (Fig. 2e) in order to determine its vertical position in the trap. This position is stabilized by feeding back the vertical position information to the DC voltage applied to the endcap electrodes. From the magnitude of this voltage, the mass-to-charge ratio of the droplet can be deduced. This value serves to adjust the frequency of the AC voltage to assure stable trapping as the droplet evaporates. Under typical conditions, this frequency varies between 200 Hz and 500 Hz. Laser light scattered from the droplet under $90° \pm 5°$ is collected by a second microscope objective and imaged onto a photomultiplier tube (Fig. 2f). Its signal serves to control the amplitude of the forced quadrupole oscillation of the droplets in the field of the trap and also provides the $t = 0$ signal at the onset of the instability which is used to trigger the flashlamp and the microscope camera after a predefined delay Δt for the ultrafast photography experiments. Figure 3a shows the photomultiplier signal

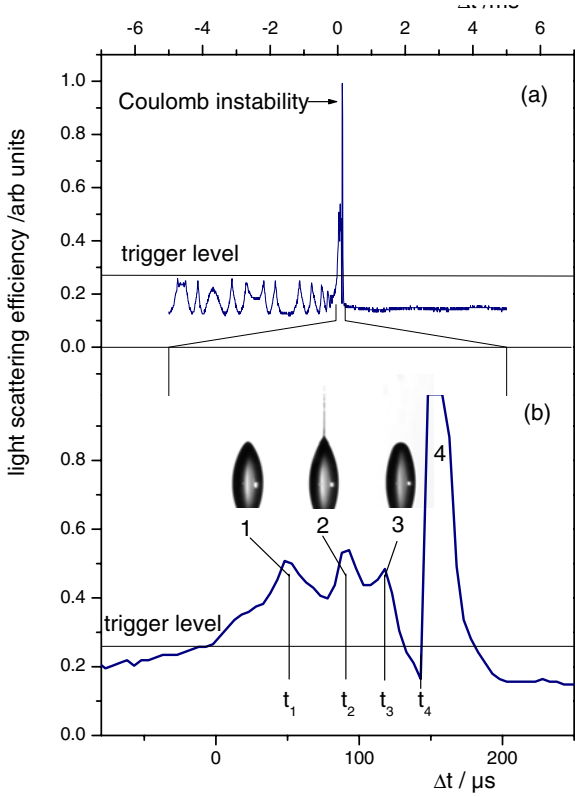

Fig. 3. Time resolved light scattering efficiency of a levitated droplet around the Coulomb instability. (a) Overview, (b) fine structure of peack around $t = 0$.

around a Coulomb instability. In the time interval prior to the instability ($t < 0$), the signal is modulated due to the large amplitude quadrupole oscillation of the droplets [7]. The onset of the instability is marked by a pronounced increase in light scattering efficiency, which is used to define $t = 0$ before the signal drops back to the level typical for spherical droplets at $t > 0$, but now it is much less modulated due to the lower amplitude of quadrupole oscillation at lower fissility. The central peak exhibits some distinct fine structure which becomes visible in Figure 3b where four relative maxima (labeled 1−4) are easily discernible. The last large maximum (4) is related to the firing of the flash lamp which saturates the photomultiplier tube. By setting the flashlamp delay (t_4) to the corresponding times, we are able to explore the droplet shape at the three intermediate maxima (1, 2 and 3) and find that the central maximum is related to the moment of jet formation, while the first and the last maximum are related to highly prolate shapes before and after the charge ejection (insert in Fig. 3b). This offers a convenient way to deduce the time necessary from the onset of the instability to the jet formation just from analyzing the light scattering trace.

3 Results

In our experiments droplets of ethylene glycol and glycerol have been investigated at temperatures between room temperature and 370 K. Due to the strong dependence of

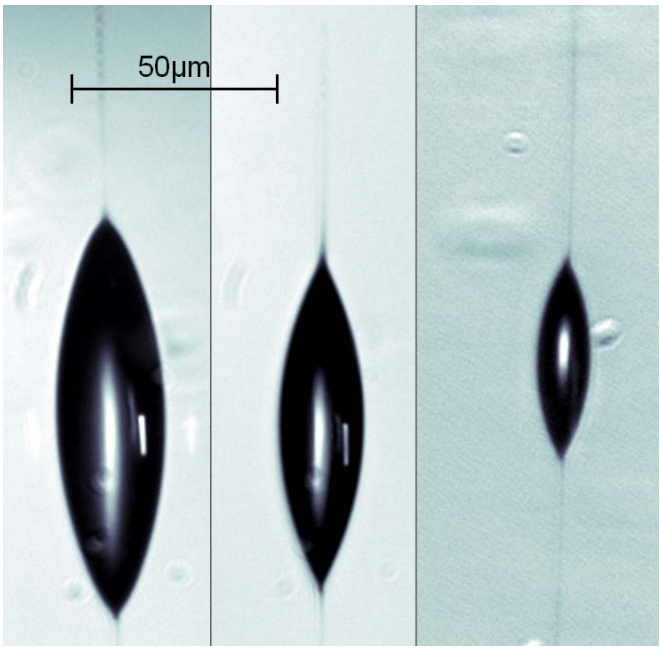

Fig. 4. Ethylene glycol droplets of various sizes at the moment of Coulomb instability.

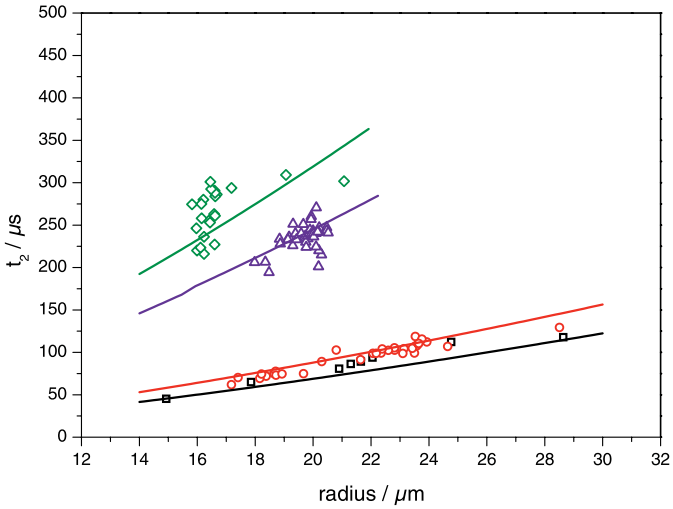

Fig. 5. Observed times t_2 for jet formation as a function of droplet size and viscosity (symbols) together with power law curves (straight lines, cf. text); (a) squares: glycol, T = 304.3 K, η = 13.5 mPa s, (b) circles: glycol, T = 300.1 K, η = 15.8 mPa s, (c) triangles: glycerol, T = 358.9 K, η = 27.1 mPa s, (d) diamonds: glycerol, T = 351.1 K, η = 35.5 mPa s.

the evaporation speed on the temperature, glycol droplets had to be investigated around room temperature while glycerol droplets had to be investigated around 360 K. At these elevated temperatures the droplets become somewhat disturbed by convective air flow which explains the larger scatter of the data in this case. These constraints limit the range of viscosity to 13 mPa s $< \eta <$ 35 mPa s while the radius a_0 at instability of the investigated droplets ranged between 14 μm and 29 μm. We found that in this size and viscosity range for both liquids the droplet shape in the moment of instability is very similar and does not change with size or temperature. This is illustrated in Figure 4 where glycol droplets of different sizes are shown in the moment of jet formation. Very similar but lower quality images have been obtained for glycerol. The spindle like shapes with full tip opening angles of 60° and an aspect ratio of about 3.5 seem to be universal for Rayleigh jet formation. The time t_2 needed for jet formation on the other hand is a strong function of both size and viscosity of the droplets. This is illustrated in Figure 5, where t_2 for glycol and glycerol droplets at room temperature is given as a function of the radius of the droplet at the onset of instability. Similar experiments were repeated at elevated temperature and with glycerol droplets. The results are included in Figure 5. We find that t_2 is also strongly dependent on the viscosity η, the higher η, the longer t_2. If we assume that the dependence of t_2 on a_0 and η can be described by a power law in the form

$$t_2 = C\, a_0^{\alpha}\, \eta^{\beta} \qquad (1)$$

then we can determine the exponents by fitting equation (1) to the data points in Figure 5 and arrive at $\alpha = 1.42 \pm 0.1$ and $\beta = 1.61 \pm 0.2$ (solid lines in Fig. 5).

Within the limit of error, both exponents are compatible with the assumption $\alpha = \beta = 3/2$, which seems to be justified at least for α, as for multipole droplet vibrations the period scales with $a_0^{3/2}$ [15]. We hope that these results will help in the understanding of the complex hydrodynamics of the Rayleigh jet formation.

We thank Bernd A. Huber for ongoing discussions and cooperation. This work was funded partially by the Deutsche Forschungsgemeinschaft (DFG) under Grant No. LE834/1.

References

1. Lord Rayleigh, Phil. Mag. **14**, 184 (1882)
2. G.I. Taylor, Proc. R. Soc. London Ser. A **280**, 383 (1964)
3. M.A. Abbas, J. Latham, J. Fluid Mech. **30**, 663 (1967)
4. J.W. Schweizer, D.N. Hanson, J. Coll. Inter. **35**, 417 (1971)
5. D.C. Taflin, T.L. Ward, E.J. Davis, Langmuir **5**, 376 (1989)
6. A. Gomez, K. Tang, Phys. Fluids **6**, 404 (1993)
7. D. Duft, H. Lebius, B.A. Huber, C. Guet, T. Leisner, Phys. Rev. Lett. **89**, 084503 (2002)
8. D. Duft, T. Achtzehn, R. Müller, B.A. Huber, T. Leisner, Nature **421**, 128 (2003)
9. R.L. Grimm, J.L. Beauchamp, J. Phys. Chem. B. **107**, 14161 (2003)
10. P.R. Brazier-Smith, S.G. Jennings, J. Latham, Proc. R. Soc. Lond. A **325**, 363 (1971)
11. P.M. Adornato, R.A. Brown, Proc. R. Soc. Lond. A **389**, 101 (1983)
12. J.A. Tsamopoulos, T.R. Akylas, R.A. Brown, Proc. R. Soc. Lond. A **401**, 67 (1984)
13. E. Fischer, Z. Physik **156**, 1 (1959)
14. R.F. Wuerker, R.V. Langmuir, Appl. Phys. **30**, 342 (1959)
15. R.W. Hasse, Ann. Phys. **93**, 68 (1975)